JOURNAL OF APPLIED PHYSICS VOLUME 84, NUMBER 5 1 SEPTEMBER 1998

The electronic structure and optical properties of intermixed GaAs/AlGaAs double quantum wells

Maolong Ke, A. Saher Helmy, A. C. Bryce, and J. H. Marsh
Department of Electronics and Electrical Engineering, University of Glasgow, Glasgow, G12 8QQ, United Kingdom

J. Davidson and P. Dawson
Department of Physics, University of Manchester Institute of Science and Technology, Manchester, M60 1QD, United Kingdom

(Received 10 March 1998; accepted for publication 26 May 1998)

We report photoluminescence and photoluminescence excitation (PLE) investigations of intermixed GaAs/AlGaAs double quantum wells. The PLE spectra provide energy information about many different transitions, from which the band profile can be more reliably derived. Using the widely assumed error function profile, it was not possible to explain the observed results. Detailed analysis revealed that the as-grown sample had a graded interface which affected the band profile for the intermixed samples. © *1998 American Institute of Physics.* [S0021-8979(98)03917-6]

I. INTRODUCTION

There is currently intense interest in monolithic integration of semiconductor lasers, low loss waveguides, phase modulators, and other components.[1,2] The crucial challenge in integration is to produce different optical and electronic properties at different regions within the same wafer. Two approaches have been devised and pursued independently to this end. One is through regrowth or even multiple growths.[3] Such an approach is obviously expensive and inconvenient, and unsuitable for some material systems, particularly Al-containing alloys, due to the difficulty of growing on an oxidized surface. The other approach is through postgrowth intermixing or interdiffusion.[4,5] The advantage of such a technique over its regrowth rival is convenience and low cost, and also compatibility with other fabrication processes. Many different methods have been developed over the years in order to improve the optical properties of the intermixed layer and the interface abruptness between the intermixed and the control regions. Recent reports have shown that the optical loss in the intermixed passive section is reduced to a level purely resulting from fundamental free carrier absorption in the doped cladding regions.[4,6] The intermixing itself does not seem to lead to any optical loss, suggesting that the intermixing approach has reached a new phase in its development and is truly advantageous over the regrowth technique.

An error function approach has been used by several groups to predict the electronic band profile of the intermixed quantum well region.[7,8] However, experimental support has so far mostly been limited to studies of the lowest band edge transition, namely the lowest electron state to the highest hole state (E1-HH1). As has been pointed out in a purely theoretical paper by E. H. Li,[7] the subband edge energies do not behave in a uniform fashion with intermixing, suggesting that when only the lowest interband energy is used to characterize the intermixing process, errors are likely to occur.

In this article we report a more detailed analysis of the band profile in an intermixed double quantum well structure and show that analysis of the transition energies from several subbands, instead of only the lowest transition energy, gives improved knowledge about the interface abruptness in the as-grown epitaxial structure. The material structure used was grown by metal organic vapour phase epitaxy (MOVPE) and consisted of an undoped 0.23 μm thick $Al_{0.2}Ga_{0.8}As$ core containing two 10 nm thick GaAs quantum wells (QWs), separated by a 10 nm thick $Al_{0.2}Ga_{0.8}As$ barrier. The core was sandwiched between a 1.5 μm thick $Al_{0.4}Ga_{0.6}As$ lower cladding layer (*n*-type doped, 10^{18} cm^{-3}, Si) and a 0.9 μm thick $Al_{0.4}Ga_{0.6}As$ upper cladding layer (*p*-doped, 5×10^{17} cm^{-3}, C). A 0.1 μm thick highly *p*-doped (8×10^{18} cm^{-3}, Zn) GaAs contact layer completed the structure. Intermixing was achieved using a well developed process known as impurity free vacancy disordering (IFVD).[8]

II. RESULTS AND DISCUSSION

Both low temperature photoluminescence (PL) and photoluminescence excitation (PLE) measurements were performed on a set of intermixed samples and an as-grown reference sample. Figure 1 shows the PL and PLE data obtained from three representative layers. A He–Ne laser was used for the PL measurement and Ti-sapphire laser for PLE. From the PL data [Fig. 1(a)], it is clear that the lowest band edge transition energy increases with intermixing, which is also confirmed by the PLE data [Fig. 1(b)] where the lowest peak represents the E1-HH1 excitonic transition. Many other transitions are also visible in the PLE spectra, which provide rich information on the effects of the intermixing on the higher lying subbands. The transitions are marked with a set of capital letters (A,B,C,D,E,F) and their likely origins, based on our simulation results, are shown in Table I. The Ti-sapphire laser used had a cutoff energy of about 1.62 eV, so transitions higher than that were unobservable. It is clear

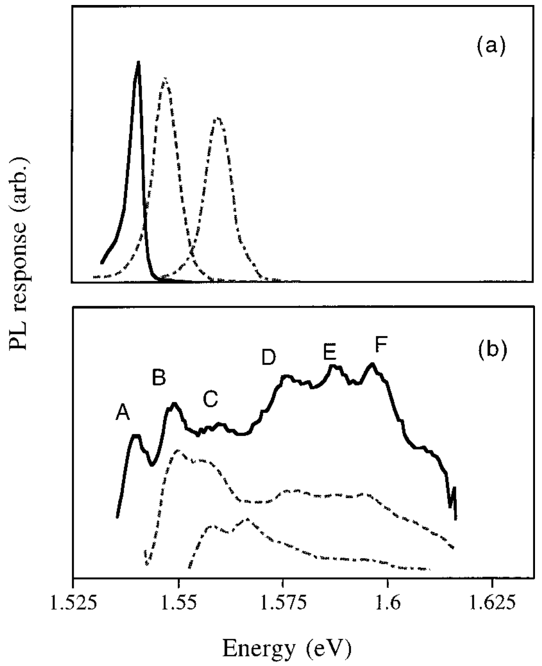

FIG. 1. (a) Low temperature PL data obtained from the as-grown reference sample (solid line), and samples intermixed at 925 °C for 15 s (dashed line), intermixed at 925 °C for 60 s (dash-dotted line). (b) The corresponding PLE data.

from the spectra that some of the higher energy peaks do not increase in energy while the lower ones do. We shall return to this later in more detail.

The electronic band profile of the as-grown sample had initially been calculated through a finite difference method by assuming a square well shape. The model and parameters used here are similar to those in our earlier publications.[9,10] A conduction band offset of 0.65 ΔE_g was used and nonparabolicity was included following Ekenberg.[11] The electron band edge effective mass was 0.0665 m_o, while the Luttinger parameters, as formulated by Lawaetz, were used to derive the heavy and light hole masses.[12] An exciton binding energy of 10 meV, a value well supported in literature,[13] was used for calculating the various transition energies. Table I shows the transition energies from both the simulated and PLE data (columns 2 and 3). While the two sets of data agree well for the lower transitions, there is, however, a noticeable discrepancy for the higher ones. The calculated energies for the higher subbands always appear to be larger than those observed experimentally, suggesting a wider well is needed for the higher subband. Similar behavior has very recently been reported by another group,[14] who suggested an exponential profile for their as-grown MOVPE AlGaAs/GaAs QWs instead of normal rectangular/square wells.

TABLE I. The experimentally observed transition energies for an as-grown (nonintermixed sample) (column 2). The calculated results are shown assuming both a square well (column 3) and an exponential well profile (column 4).

Transition	E_{exp} (eV)	E_{cal} Square well (eV)	E_{cal} Exponential well (eV)
E1-HH1 (A)	1.539	1.541	1.537
E1-LH1 (B)	1.549	1.551	1.547
E1-HH2 (C)	1.560	1.563	1.558
E1-HH3 (D)	1.576	1.586	1.579
E2-HH1 (D)	1.576	1.587	1.578
E1-LH2 (E)	1.588	1.604	1.590
E2-LH1 (E)	1.588	1.602	1.589
E2-HH2 (F)	1.597	1.616	1.598

The following exponential profile was used to describe the Al concentration in the as-grown sample,

$$X = X_o \exp[-\beta/(z^2-(L_w/2)^2)] \quad \text{for } |z| \geqslant L_w/2, \qquad X=0 \quad \text{for } |z| \leqslant L_w/2, \tag{1}$$

where X_o is the nominal Al content (0.2), β the curvature parameter, and 3.5 (nm^2) was used here, and L_w the initial well width (10 nm) or the width of the bottom of the well. Using Eq. (1) a much better fit for all the transition energies was obtained as shown in Table I (columns 2 and 4). We have also attempted to use an error function to fit the data for the as-grown sample but no suitable match could be found.

This graded initial interface is obviously going to influence the final shape of the intermixed wells. It is assumed Fick's second law still dictates the interdiffusion between the Ga and Al during intermixing,

$$\frac{dX}{dt} = D\,\frac{d^2X}{dz^2}, \tag{2}$$

where D is the diffusion coefficient. If the initial condition is a square well, the Al concentration can be obtained as

$$X(z) = \frac{Xo}{2\sqrt{\pi Dt}} \int_{(Lw/2)-z}^{\infty} \exp\left(\frac{-\eta}{4Dt}\right) d\eta + \frac{Xo}{2\sqrt{\pi Dt}} \int_{(Lw/2)+z}^{\infty} \exp\left(\frac{-\eta}{4Dt}\right) d\eta \tag{3}$$

leading to the well known error function profile. However, when the initial Al concentration profile is an exponential function $f(z)$, the solution of the diffusion equation is now given by

$$X(z) = \frac{Xo}{2\sqrt{\pi Dt}} \int_{(Lw/2)-z}^{\infty} f(\eta)\exp\left(\frac{-\eta}{4Dt}\right) d\eta + \frac{Xo}{2\sqrt{\pi Dt}} \int_{(Lw/2)+z}^{\infty} f(\eta)\exp\left(\frac{-\eta}{4Dt}\right) d\eta. \tag{4}$$

This equation can only be solved numerically. It is easy to see that, when $f(\eta)=1$, the above equation reverts to the square well form.

Figure 2 shows our calculated potential profiles from the initially graded interface. The main difference between these profiles and the profiles obtained from the error function approach was that the upper part of the well was effectively much wider for the exponential profile. Figure 3 displays calculations of two representative subband edge energies for different diffusion lengths. The solid lines were calculated using the new formula (4) while the dashed lines were calculated using the error function approximation (3). The ex-

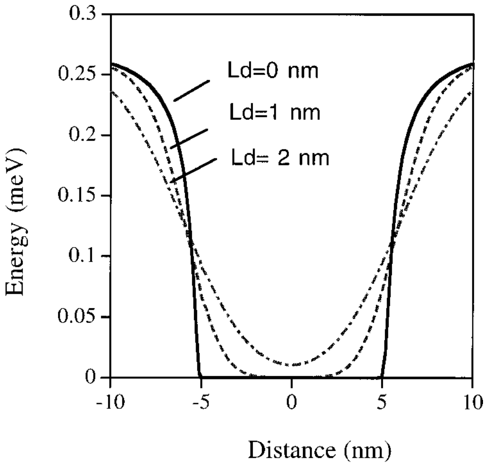

FIG. 2. Conduction band potential profile for different diffusion lengths obtained using the newly derived formula.

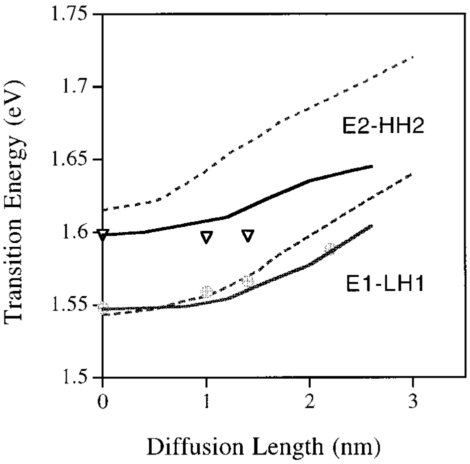

FIG. 3. Calculated transition energies for E1-LH1 and E2-HH2 from the new formula (solid lines) and the error function approach (dashed lines). Experimental data are also displayed with ⊕ for E1-LH1 and ∇ for E2-HH2.

perimental data are also displayed for comparison. Clearly, the solid lines compare much more closely with the experimental data than the dashed ones.

Another interesting result from the PLE data is that many of the observed transitions are in fact ''forbidden.'' It is well known that, under an ideal infinitely deep square well condition, only transitions with $\Delta l = m - n = 0$, where m and n are the subband indices of the conduction and valence bands, respectively, are allowed because the wave functions of all other transitions are exactly orthogonal. However, for a real QW which has a finite depth and may contain graded interfaces like here, the orthogonality of the wave functions is relaxed, resulting in a modified selection rule, where Δl $=$even transitions are allowed. This is why transitions, like E1-HH3, have been widely observed in absorption or excitation spectra.[15] In the case of the laser structure studied here, the p- and n-type dopants lead to breaking in potential symmetry, the $\Delta l =$even selection rule is also violated and virtually all the possible transitions become allowed.

III. CONCLUSION

In summary, we have reported, to our best knowledge, the first PLE data from a set of IFVD intermixed GaAs/AlGaAs double quantum wells. Many subband transitions were observed and detailed comparison with simulation results revealed that the as-grown sample had a graded interface which can be described to a good approximation as exponential. This grading has been found to influence substantially the band profile after intermixing. A generalized formula for working out the intermixed Al concentration, which can be applied to any initial graded interface (boundary condition), has been derived, and numerically calculated results using the new formula were found to be in better agreement with our experimental observation than the error function approach.

ACKNOWLEDGMENTS

The authors would like to acknowledge the financial support from the U. K. Engineering and Physical Sciences Research Council. The U. K. Ministry of Defense is also gratefully acknowledged.

[1] J. H. Marsh and A. C. Bryce, Mater. Sci. Eng., B **24**, 272 (1994).
[2] J. Werner, T. P. Lee, E. Kapon, E. Colas, N. G. Stoffel, S. A. Schwarz, L. C. Schwartz, and N. C. Andreadakis, Appl. Phys. Lett. **57**, 810 (1990).
[3] M. Aoki, H. Sano, M. Suzuki, M. Takahashi, K. Uomi, and A. Takay, Electron. Lett. **27**, 2138 (1990).
[4] B. S. Ooi, K. McIlvaney, M. W. Street, A. S. Helmy, S. G. Ayling, A. C. Bryce, J. H. Marsh, and J. S. Roberts, IEEE J. Quantum Electron. **33**, 1784 (1997).
[5] W. D. Laidig, N. Holonyak, Jr., M. D. Camras, K. Hess, J. J. Coleman, P. D. Dapkus, and J. Bardeen, Appl. Phys. Lett. **38**, 776 (1981).
[6] S. D. McDougall, O. P. Kowalski, C. J. Hamilton, F. Camacho, B. C. Qiu, M. L. Ke, R. M. De La Rue, A. C. Bryce, and J. H. Marsh, IEEE J. Selected Topics Quantum Electron. (unpublished).
[7] E. H. Li, B. L. Weiss, and K. S. Chan, Phys. Rev. B **46**, 15 181 (1992).
[8] I. Gontijo, T. Krauss, J. H. Marsh, and R. M. De La Rue, IEEE J. Quantum Electron. **QE-30**, 1189 (1995).
[9] M. L. Ke and B. Hamilton, Phys. Rev. B **47**, 4790 (1993).
[10] M. L. Ke, J. S. Rimmer, B. Hamilton, J. H. Evans, M. Missous, K. E. Singer, and P. Zalm, Phys. Rev. B **45**, 14 114 (1992).
[11] U. Ekenberg, Phys. Rev. B **36**, 6152 (1987).
[12] P. Lawaetz, Phys. Rev. B **4**, 3460 (1971).
[13] See, for example, P. Dawson, K. J. Moor, G. Duggan, H. I. Ralph, and C. T. B. Foxon, Phys. Rev. B **34**, 6007 (1986).
[14] W. C. H. Choy, P. J. Hughes, and B. L. Weiss, Mater. Res. Soc. Symp. Proc. **450**, 425 (1997).
[15] See, for example, C. Delalande, G. Bastard, J. A. Brum, H. W. Liu, M. Voos, G. Weimann, and W. Schlapp, Phys. Rev. Lett. **59**, 2690 (1987).